JOURNAL OF SYNCHROTRON RADIATION
ISSN 1600-5775

Applications of VUV extra-focus mechanism: high-performance dual-mode monochromator from VUV to soft X-ray

Chaofan Xue, Yanqing Wu,* Ying Zou, Lian Xue, Zhi Guo, Yong Wang* and Renzhong Tai*

Shanghai Institute of Applied Physics, Chinese Academy of Sciences, Shanghai Synchrotron Radiation Facility, Shanghai, 201800, People's Republic of China. *Correspondence e-mail: wuyanqing@sinap.ac.cn, wangyong@sinap.ac.cn, tairenzhong@sinap.ac.cn

Received 12 February 2015
Accepted 19 August 2015

Edited by G. E. Ice, Oak Ridge National Laboratory, USA

Keywords: ultra-wide energy range; CIA-VCGM; VIA-VPGM.

A new monochromator scheme is presented in which an extra-focus constant-included-angle varied-line-spacing cylindrical-grating monochromator (extra-focus CIA-VCGM) is conveniently combined with a variable-included-angle varied-line-spacing plane-grating monochromator (VIA-VPGM). This dual-mode solution delivers high performance in the energy range from vacuum ultraviolet (VUV) to soft X-ray. The resolving power and the efficiency of this dual-mode grating monochromator are analyzed in detail based on realistic parameters. Comparisons with the commonly used variable-included-angle plane-grating monochromator and normal-incidence monochromator (VIA-PGM/NIM) hybrid monochromator are made.

1. Introduction

For beamline design, the covered energy range is an important parameter, which is determined by its scientific goals. As is well known, the angle-resolved photoemission spectroscopy (ARPES) method is a significant technique addressing electron properties close to the Fermi surface in materials (Tanaka *et al.*, 2006; Terashima *et al.*, 2006; Damascelli *et al.*, 2003). For ARPES, the escape depth of photoelectrons emitted from solid materials exhibits the famous 'V-curve' dependence on kinetic energy (Somorjai, 1981). If the work function of a material is taken into account, the escape depth reaches below 1 nm in the photon energy range 10–200 eV, which enhances surface sensitivity yet limits the ability to obtain bulk information from a sample. For some samples it is vital to know both their surface and their bulk information *in situ* without suspicious property change caused by reloading at alternative beamlines. This can be achieved if the energy range for a soft X-ray monochromator can be extended down to 7 eV. Such a vacuum ultraviolet (VUV) extension can play a dramatic role in the experiment; the escape length can be longer than 10 nm. Consequently, both surface and bulk information of the same position in a sample can be obtained in one endstation at the same beamline.

Among various kinds of soft X-ray monochromators, a hybrid monochromator, which is a combination of a variable-included-angle plane-grating monochromator (VIA-PGM) and a normal-incidence monochromator (NIM), has been known to offer a broad energy range from VUV to soft X-ray with a decent performance. The VIA-PGM (Petersen, 1982), which has been employed at many synchrotron radiation

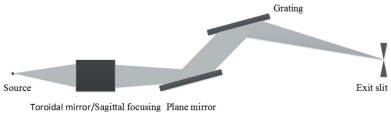

beamlines (Xue *et al.*, 2010; Aksela *et al.*, 1994; Follath, 2001; Warwick *et al.*, 2001; Follath *et al.*, 1998, Follath & Senf, 1997) all over the world, is one of the most successfully developed optics of the last few decades. There are numerous advantages of this monochromator. Besides covering a wide energy range, the VIA-PGM can operate in different modes, such as high-energy resolution, higher-order harmonic suppression and high-flux modes, by selecting a suitable C_{ff} (fixed-focus constant) value. Furthermore, a variable-line-space (VLS) plane grating is applied in some new VIA-PGMs called VIA-VPGMs (Xue *et al.*, 2014; Reininger & de Castro, 2005; Ono *et al.*, 2004; Amemiya *et al.*, 2010), which is a significant improvement with respect to the original design. By using the VLS grating, the beam can be focused at the exit slit at any included angle, without introducing coma and spherical aberration into the system. Even though the VIA-PGM can cover a wide energy range, it is almost all in the soft X-ray range (above 20 eV). This type of monochromator is difficult to extend to energies in the VUV range (<7 eV) while keeping good energy resolution. It is mainly constrained by the mechanical limits of the rotation angles for the plane mirror and the gratings, and the geometrical size of the plane mirror (Follath, 2001). A low line density grating is employed to cover the low-energy end because the diffraction angle of the low line density grating is relatively large; either blocking of the incoming beam or colliding with the mirror by the grating can be avoided while the performance of the monochromator is not harmed. In addition, the fact that the beam no longer hits the grating center in the VUV range causes energy drift. A normal-incidence monochromator is a remedy. It was proposed to combine it with the VIA-PGM to extend the energy range to the VUV (Flechsig *et al.*, 2001; Follath & Schmidt, 2004; Borisenko, 2012) while the exit slit would stay fixed. In NIM mode, however, the photon flux is low due to the very small incident angle. Moreover, the alignment of a monochromator in NIM mode is challenging because of the long distance between the pre-mirror and the grating, a mechanical compatibility problem between the two modes.

An extra-focus constant-included-angle varied-line-spacing cylindrical-grating monochromator (extra-focus CIA-VCGM) based on the Hettrick–Underwood scheme has been described in our previous work (Xue *et al.*, 2015). By replacing the plane grating in a standard CIA-PGM monochromator with a cylindrical one, the defocus aberration of such an extra-focus CIA-VCGM can be optimized at three reference photon energies rather than two reference photon energies of the Hettrick–Underwood scheme in the VUV range. Thanks to its strong focusing ability, a fixed focus spot can be obtained with retained high performance, though the monochromator is operated in the constant-included-angle (CIA) mode. Compared with a NIM, both its photon flux and its energy resolution are increased because it is a grazing-incidence monochromator, similar to a 'dragon'-type monochromator. Furthermore, this monochromator has a simple mechanical structure and its mechanical compatibility with a standard varied-line-spacing plane-grating monochromator (VPGM) allows convenient extension into the soft-X-ray range.

In this study a dual-mode VLS grating monochromator (DM-VGM) is proposed. The new monochromator combines the extra-focus CIA-VCGM and the VIA-VPGM to cover an energy range from VUV to soft X-ray while maintaining high performance over the whole range.

2. Layout and performance of the DM-VGM

2.1. Monochromator layout and operation mode

For the VIA-VPGM, two optical elements are needed: an off-center rotation mirror to change the included angle and a grating to diffract the beam. For the extra-focus CIA-VCGM, there are two possible arrangements: meridional focusing scheme and sagittal focusing scheme (Xue *et al.*, 2015). It turns out that the latter is suitable for combining with the VIA-VPGM because the beam focusing condition will not be affected when the grating included angle is changed by the additional plane mirror. The layout of the new monochromator, DM-VGM, is shown in Fig. 1. Three optics are necessary for the new monochromator: (i) a sagittal focusing mirror (cylindrical or toroidal mirror), demanded by the extra-focus CIA-VCGM, is employed to converge the beam in the dispersion direction; the beam can be focused to the exit slit in the non-dispersion direction if the mirror is a toroidal one; (ii) a plane mirror is applied to change the included angle; (iii) a set of gratings with different surface figures is used to diffract the beam for different operation modes. The DM-VGM combines two types of gratings for different operating modes: a plane grating for VIA-VPGM mode (VIA mode) and a cylindrical grating for extra-focus CIA-VCGM mode (CIA mode). Note that the mechanical structure of a DM-VGM is similar to a conventional VIA-VPGM, which makes the combination of these two modes highly compatible.

In order to illustrate the performance of the new monochromator, a 4 m-long undulator is chosen as a realistic optical source and typical optical distances are assumed for a model DM-VGM. Beam sizes and divergences are calculated from

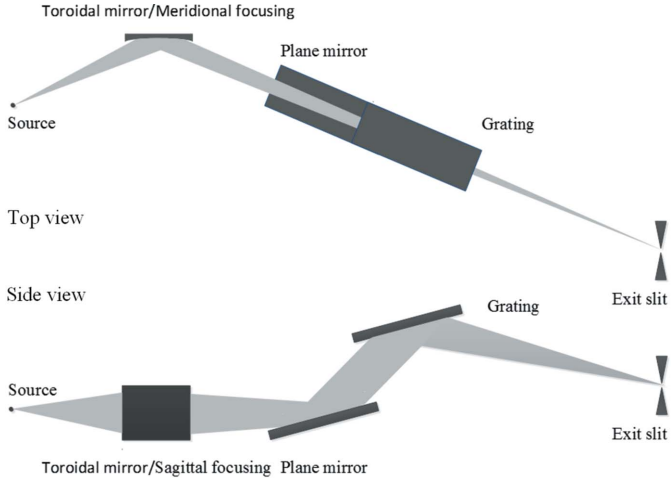

Figure 1
Layout of the new monochromator, DM-VGM.

Table 1
Detailed parameters for the calculations.

Electron beam RMS size	
Horizontal σ_x (mm)	0.15855
Vertical σ_y (mm)	0.00987
Electron beam RMS divergence	
Horizontal σ_x (rad)	3.2914×10^{-5}
Vertical σ_y (rad)	3.9497×10^{-6}
Undulator length (mm)	4000
Grating slope error (rad)	3×10^{-7}
Plane mirror slope error (rad)	5×10^{-7}
Focusing mirror slope error (rad)	2×10^{-6}
Object distance of focusing mirror (mm)	20000
Imaging distance of both gratings (mm)	13000
Distance between focusing mirror and plane mirror (mm)	13000
Total beamline length (mm)	46000
Height between incoming and outgoing beam (mm)	30.5
Grating line density (lines mm^{-1})	1000

the vector sum of the electron beam RMS values (σ_x, σ_x', σ_y, σ_y') on the orbit and the radiation values (σ_r, σ_r'). The radiation values are calculated using the approximations $\sigma_r = (2\lambda L)^{1/2}/2\pi$ and $\sigma_r' = (\lambda/2L)^{1/2}$, where λ is the wavelength of the radiation and L is the length of the insertion device. The operating energy range of either VIA mode or CIA mode is mainly confined by the mechanical limits and the performance. In the VIA mode, a higher line density grating means a smaller diffraction angle, which increases the possibility that the incoming beam will be blocked by the grating at the low-energy end, as well as a collision risk between the grating and the plane mirror. Such problems can be avoided by a lower line density grating at a price of too low-energy resolution, which might not meet the experimental requirements. Therefore, at the low-energy VUV end, it is better to engage the CIA mode as the diffraction angle for the extra-focus CIA-VCGM is larger than that of the VIA-VPGM, and thus a high line density grating can be employed to ensure a high-energy resolution. Detailed parameters used in the calculations are listed in Table 1.

An optimal distance between the focusing mirror and the plane mirror can be found to confine the beam footprint on the grating so as to reduce the risk of the grating blocking the incoming beam or colliding with the plane mirror. As shown in Table 1, for a mode example the object distance of the focusing mirror is 20 m and the distance between the focusing mirror and the plane mirror is 13 m. Under such conditions the beam size is about 8 mm and the maximum footprint on the grating is about 69 mm. With a 10 mm margin on both sides of the grating, the incoming beam will not be blocked by the grating in the whole energy range as long as the diffraction angle is larger than 53.64° which is the minimum angle allowed. Thanks to a large included angle in the CIA mode, the diffraction angle is larger than the minimum allowed angle as shown in Fig. 2.

The choice of the reference energies for the CIA mode is not arbitrary in the DM-VGM because it determines the position of the grating virtual source and then the beam footprint on the grating. For the model DM-VGM in this study the reference energies are chosen to be 7 eV, 8 eV and 12 eV, and the coma aberration vanishes at 7 eV. For the VIA mode, the C_{ff} value is set to be 5 at 120 eV, which takes account of the energy resolution and the footprint on the grating, and the coma aberration vanishes at 60 eV. A few parameters can be derived under these conditions and are listed in Table 2.

Table 2
Derived parameters for the model DM-VGM.

	CIA mode	VIA mode
b_2 (mm^{-1})	0.000121031	0.000155628
b_3 (mm^{-2})	3.06509×10^{-9}	6.4273×10^{-9}
Virtual source of grating (mm)	22207	22207
Curvature radius of focusing mirror (mm)	668	668
Curvature radius of grating (mm)	190460	–

Table 3
Comparison of the difference of optical parameters between the CIA mode and the extra-focus CIA-VCGM in our previous work.

	CIA mode in DM-VGM	Extra-focus CIA-VCGM
Optimized energy (eV)	7, 8, 12	7, 8.5, 25
Included angle (°)	138	140
Focusing mirror		
Object distance (mm)	20000	20000
Curvature radius (mm)	765	729
Deflect angle (°)	3	3
Cylindrical grating		
Imaging distance (mm)	13000	29000
Curvature radius (mm)	190460	497663
b_2 (mm^{-1})	0.000121031	5.56311×10^{-5}
b_3 (mm^{-2})	3.06509×10^{-9}	7.19823×10^{-10}

Although the principle is the same, the optical parameters for an extra-focus CIA-VCGM can vary under different conditions. In our previous work the monochromator can be optimized with few constraints. However, in this study there are more constraints for optimizing the CIA mode because the VIA mode has to be optimized as well. The optical parameters of the extra-focus CIA-VCGM in our previous work and of the CIA mode in this study are listed in Table 3 for comparison.

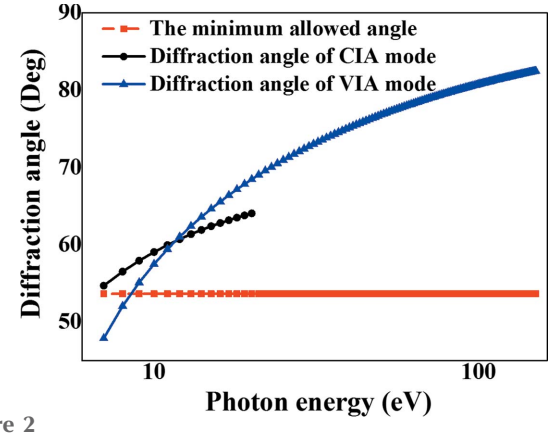

Figure 2
Diffraction angles of the two different operating modes. The line density of both grating is 1000 lines mm^{-1} and +1st order diffraction is considered.

2.2. Energy resolution

At the low-energy end, the included angle is much larger in the CIA mode than in the VIA mode, as shown in Fig. 3(*a*). A larger included angle allows a higher grating line density and a higher C_{ff} value, promising a higher energy resolution. It is noted that in the different operation mode the C_{ff} value shows an opposite trend with energy: decreasing in the CIA mode but increasing in the VIA mode, as shown in Fig. 3(*b*). For this model DM-VGM, a transition point occurs at 11.6 eV, at which the C_{ff} values of the two operation modes are equal. The energy resolution of the model DM-VGM is shown in Fig. 3(*c*). It is apparent that the CIA mode can work well in the range below the transition point, and the VIA mode is better for the range above the transition point.

The energy-resolving power calculated in this study is mainly determined from seven factors: source size, exit slit size, meridian slope error of the grating and the focusing mirrors, aberrations from the defocus and the coma, and the grating diffraction limit. Fig. 4 shows their contributions to the relative spectrum width (RSW) in the two operation modes.

As seen from the figure, the largest contributions to the total energy resolving power are from the source size and the exit slit size in both operation modes. The contribution from the source size is equal to that from the exit slit size because the exit slit is variable, which is set according to the beamline demagnification, through which the beam with an FWHM cross section is allowed to pass. The second largest contribution to the RSW is from the diffraction limit. Thanks to a large C_{ff} value at the low-energy end in the CIA mode and at the high-energy end in the VIA mode, the contribution from the diffraction limit does not degrade the energy resolution severely, although the beam footprint on the grating is relatively small compared with an unfocused incoming beam. The third largest contribution to the RSW is from the slope errors of the grating and the mirrors. The above three contributions are related to the incidence/diffraction angle, so they vary with the C_{ff} value. The contributions from the aberrations are smaller than that of the above factors. For the VIA mode, there is no contribution from the defocus aberration because the defocus aberration can be zeroed over the whole energy range. For the CIA mode, the defocus aberration vanishes only at the reference energies but the contribution from the defocus aberration is still small enough to be negligible in the operated energy range.

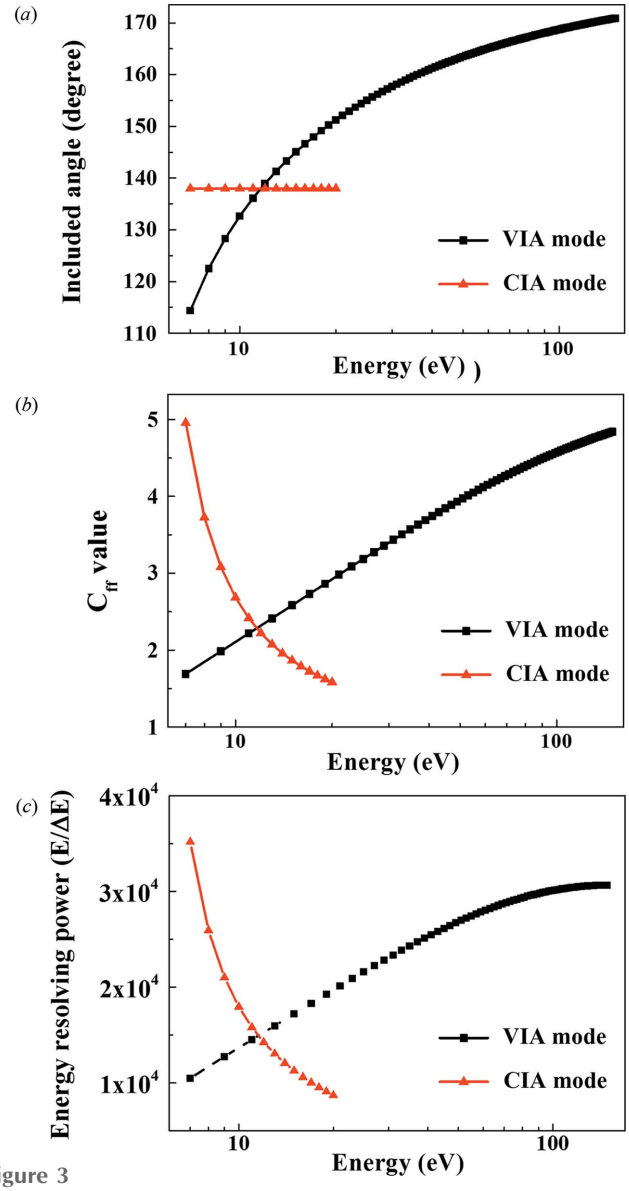

Figure 3
(*a*) Included angle, (*b*) C_{ff} value and (*c*) theoretical energy-resolving power of the model DM-VGM.

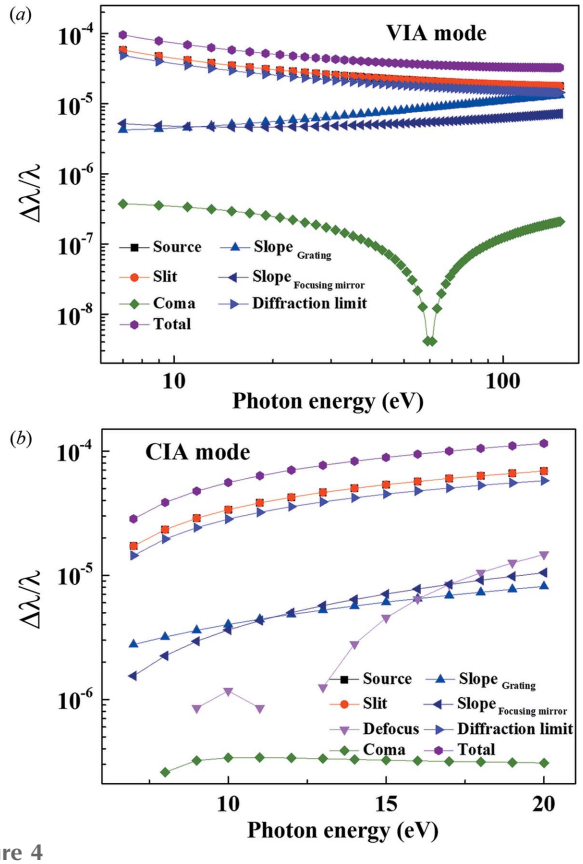

Figure 4
The various contributions to the relative spectrum width in (*a*) VIA mode and (*b*) CIA mode.

In general, the energy resolution of the DM-VGM is decided by different operating modes. High-energy resolving power can be obtained at the low-energy end by the CIA mode and at the high-energy end by the VIA mode. Because of the strong focusing ability of the extra-focus CIA-VCGM, the exit slit stays fixed even if it is operating in the CIA mode. By combining with the CIA-VCGM, not only is the energy range of the VIA-VPGM expanded, but also its performance is improved significantly.

2.3. Ray-tracing results

In order to verify the performance of the DM-VGM, ray tracing on the energy resolution is carried out using the *SHADOW* code (Sanchez del Rio *et al.*, 2011) including the same RMS slope errors as used in the analytical calculations. Spot patterns at the exit slit plane for 7, 9, 11.6 and 150 eV are shown in Fig. 5. As seen in the figure, each energy pair of spots is well resolved at theoretically predicted resolution. The result at 7 eV is obtained by using a cylindrical grating operated in the CIA mode while the result at 150 eV is obtained by using a plane grating operated in the VIA mode. The results at 11.6 eV are verified in both CIA and VIA mode because it is the transition point [Figs. 5(*c*) and 5(*d*)]. Additionally, the result at 9 eV in the CIA mode is demonstrated to show a negligible defocus aberration.

2.4. Grating efficiency

In order to compare the grating efficiency of the CIA-VCGM with that of NIM, the +1 order diffraction efficiency of a 1000 lines mm^{-1} grating with Au coating is calculated, as shown in Fig. 6. To maximize the efficiency, the groove depth of the grating is optimized to be 41 nm for the CIA-VCGM and 23 nm for the NIM. The grating efficiency is estimated by (Thompson *et al.*, 2009)

$$E_m = \frac{R}{m^2\pi^2}\left[1 - 2\cos Q^+ \cos(Q^- + \delta) + \cos^2 Q^+\right], \quad m = \text{odd}, \tag{1}$$

where

$$Q^{\pm} = \frac{m\pi h}{d_0}(\tan\alpha \pm \tan\beta),$$

$$\delta = \frac{2\pi h}{\lambda}(\cos\alpha + \cos\beta),$$

and α is the incidence angle of the grating, β is the diffraction angle of the grating, λ is the wavelength of the radiation, d_0 is the grating line density, h is the grating groove depth, R is the reflectance at grazing angle $(\alpha_G\beta_G)^{1/2}$,

$$\alpha_G = (\pi/2) - |\alpha|, \qquad \beta_G = (\pi/2) - |\beta|. \tag{2}$$

It can be seen from Fig. 6 that the efficiency of the CIA-VCGM is 4–5 times higher than that of the NIM in their common operating energy range of 7–20 eV. The groove width-to-period ratio r is assumed to be 0.5 here and, in fact, the groove width-to-period ratio of a real commercial grating will be also optimized near this value. The reflectivity of the

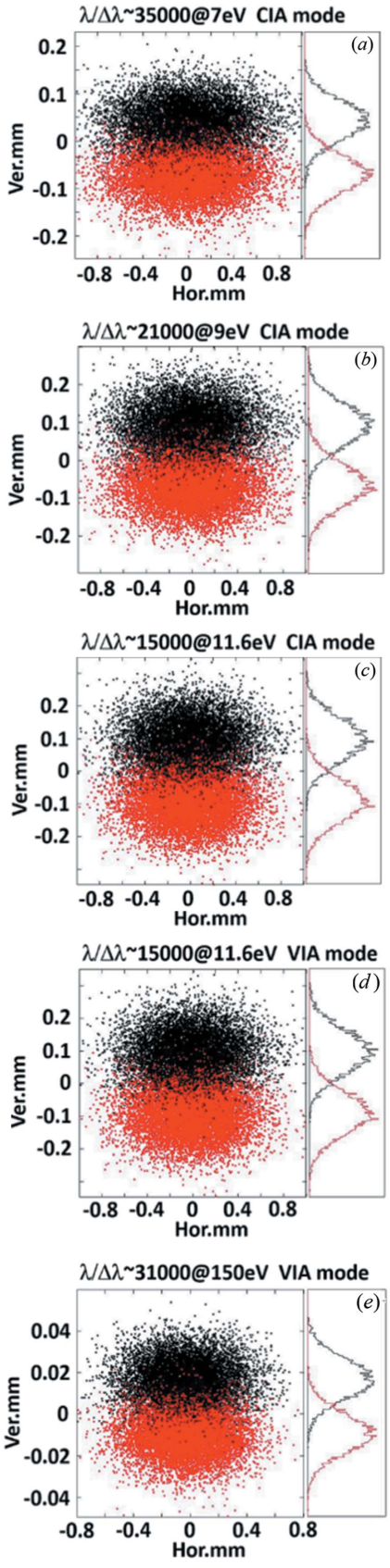

Figure 5
Ray-tracing results on the energy resolution of the monochromator at (*a*) 7 eV using cylindrical grating; (*b*) 9 eV using cylindrical grating; (*c*) 11.6 eV using cylindrical grating; (*d*) 11.6 eV using plane grating; (*e*) 150 eV using plane grating.

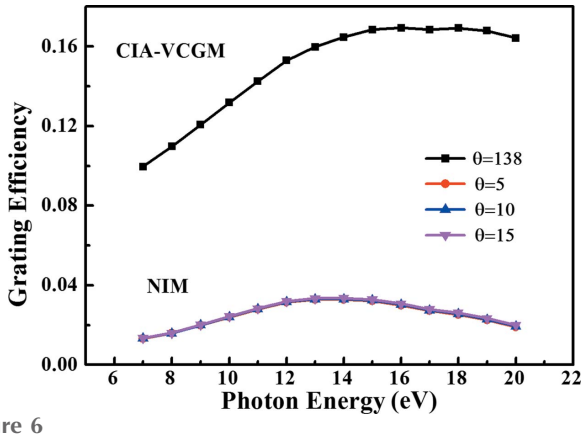

Figure 6
Comparison of first-order grating diffraction efficiency in the CIA-VCGM and NIM modes.

coating material is calculated using *XOP 2.3* code (Sanchez del Rio & Dejus, 2004).

A remark on the efficiency of a 'dragon'-type monochromator deserves to be made. Both a dragon-type monochromator and the CIA-VCGM are constant-included-angle type monochromators. The incidence angle of the mirror and the grating is the same when the constant included angle is the same. Therefore, the efficiency of either type of monochromator is almost the same.

3. Conclusion

In this study a new dual-mode monochromator (DM-VGM) for the VUV to soft X-ray energy range is presented which combines an extra-focus CIA-VCGM and a VIA-VPGM. This strategy takes advantage of the strong focusing ability of the extra-focus CIA-VCGM in the VUV range. In this scheme the mechanical structures of the CIA-VCGM and that of the PGM are compatible. The number of optical elements in such a beamline is the same as for a typical beamline with a VIA-PGM, with a converging mirror replacing the collimating/deflecting mirror to change to CIA-VCGM mode. More importantly, compared with the VIA-PGM scheme, the resolving power of our scheme in the VUV range is improved significantly thanks to a high C_{ff} value. In addition, the transmission efficiency of the newly designed monochromator is estimated to be higher than that of the NIM due to the large included angle in the VUV range. We believe that the DM-VGM monochromator will be a very attractive candidate for building a beamline for the energy range from VUV to soft X-ray. With all these advantages we believe that the DM-VGM monochromator is a promising successor for the hybrid VIA-PGM/NIM monochromator to be adopted in a new generation of beamlines for the energy range from VUV to soft X-ray, not only for new beamlines but for refurbished ones as well, due to its highly compatible mechanical structure with a conventional VIA-PGM.

Acknowledgements

This work was supported by the National Natural Science Foundation of China (No. 11205236 and No. 11275255), the Shanghai Academic Leadership Program (grant No. 13XD1404400), the National Natural Science Foundation for Outstanding Young Scientists (grant No. 11225527) and the Open Research Project of Large Scientific Facility from Chinese Academy of Sciences: Study on Self-Assembly Technology and Nanometer Array with Ultra-High Density. The authors are grateful to the staff at BL08U1B beamline (SSRF) for their help.

References

Aksela, S., Kivimäki, A., Naves de Brito, A., Sairanen, O. P., Svensson, S. & Väyrynen, J. (1994). *Rev. Sci. Instrum.* **65**, 831.
Amemiya, K., Toyoshima, A., Kikuchi, T., Kosuge, T., Nigorikawa, K., Sumii, R., Ito, K., Garrett, R., Gentle, I., Nugent, K. & Wilkins, S. (2010). *AIP Conf. Proc.* **1234**, 295–298.
Borisenko, S. V. (2012). *Synchrotron Radiat. News*, **25**, 6–11.
Damascelli, A., Hussain, Z. & Shen, Z.-X. (2003). *Rev. Mod. Phys.* **75**, 473–541.
Flechsig, U., Patthey, L. & Quitmann, C. (2001). *Nucl. Instrum. Methods Phys. Res. A*, **467–468**, 479–481.
Follath, R. (2001). *Nucl. Instrum. Methods Phys. Res. A*, **467–468**, 418–425.
Follath, R. & Schmidt, J. S. (2004). *AIP Conf. Proc.* **705**, 631–634.
Follath, R. & Senf, F. (1997). *Nucl. Instrum. Methods Phys. Res. A*, **390**, 388–394.
Follath, R., Senf, F. & Gudat, W. (1998). *J. Synchrotron Rad.* **5**, 769–771.
Ono, M., Scott, J. D. & Morikawa, E. (2004). *AIP Conf. Proc.* **705**, 360–363.
Petersen, H. (1982). *Opt. Commun.* **40**, 402–406.
Reininger, R. & de Castro, A. R. B. (2005). *Nucl. Instrum. Methods Phys. Res. A*, **538**, 760–770.
Sanchez del Rio, M., Canestrari, N., Jiang, F. & Cerrina, F. (2011). *J. Synchrotron Rad.* **18**, 708–716.
Sanchez del Rio, M. & Dejus, R. J. (2004). *Proc. SPIE*, **5536**, 171–174.
Somorjai, G. A. (1981). *Chemistry in Two Dimensions: Surfaces.* Ithaca: Cornell University Press.
Tanaka, K., Lee, W. S., Lu, D. H., Fujimori, A., Fujii, T., Risdiana, Terasaki, I., Scalapino, D. J., Devereaux, T. P., Hussain, Z. & Shen, Z.-X. (2006). *Science*, **314**, 1910–1913.
Terashima, K., Matsui, H., Hashimoto, D., Sato, T., Takahashi, T., Ding, H., Yamamoto, T. & Kadowaki, K. (2006). *Nat. Phys.* **2**, 27–31.
Thompson, A. C., Attwood, D. T., Gullikson, E. M., Howells, M. R., Kortright, J. B., Robinson, A. L., Underwood, J. H., Kim, K. J., Kirz, J., Lindau, I., Pianetta, P., Winick, H., Williams, G. P. & Scofield, J. H. (2009). *X-ray Data Booklet.* Lawrence Berkeley National Laboratory, Berkeley, CA, USA.
Warwick, T., Cambie, D., Padmore, H. A. & Howells, M. R. (2001). *Nucl. Instrum. Methods Phys. Res. A*, **467–468**, 525–528.
Xue, C. F., Wang, Y., Guo, Z., Wu, Y. Q., Zhen, X. J., Chen, M., Chen, J. H., Xue, S., Peng, Z. Q., Lu, Q. P. & Tai, R. Z. (2010). *Rev. Sci. Instrum.* **81**, 103502.
Xue, C., Wu, Y., Zou, Y., Xue, L., Wang, Y., Xu, Z. & Tai, R. (2015). *J. Synchrotron Rad.* **22**, 328–335.
Xue, L., Reininger, R., Wu, Y.-Q., Zou, Y., Xu, Z.-M., Shi, Y.-B., Dong, J., Ding, H., Sun, J.-L., Guo, F.-Z., Wang, Y. & Tai, R.-Z. (2014). *J. Synchrotron Rad.* **21**, 273–279.